An Improved MM-PO Method with UV Technique for Scattering from an Electrically Large Ship on a Rough Sea Surface at Low Grazing Angle

S. Y. He[1], C. Li[1], F. Zhang[1], G. Q. Zhu[1], W. D. Hu[2], and W. X. Yu[3]

[1] School of Electronic Information
Wuhan University, Wuhan, 430079, China
siyuanhi@gmail.com, whunpredestiny@gmail.com, zhfJoyce@hotmail.com, gqzhu@whu.edu.cn

[2] ATR Lab.
National University of Defense technology, Changsha, 410073, China
wdhu@nudt.edu.cn

[3] School of Electronic Information and Electrical Engineering
Shanghai Jiao Tong University, Shanghai, 200240, China
wxyu@sjtu.edu.cn

Abstract — An improved MM-PO-UV hybrid method is developed to calculate the bistatic scattering from the two-dimensional (2-D) composite model of an electrically large ship (ELS) on a one-dimensional (1-D) rough sea surface at a low grazing angle (LGA). The subdivision of the MM and PO region is performed flexibly according to the physical considerations. The MM region contains not only the ship but also a small portion of the neighboring sea region where the surface currents need to be modeled accurately. An iterative solution BiCGSTAB is adopted to solve the final matrix equation of a large dimension caused by the ELS. Then, a UV matrix decomposition technique is applied as the fast algorithm to accelerate the matrix-vector productions and the matrix elements filling in. The improved method makes it possible for the Monte-Carlo simulation of large-scale complex target/rough surface problems under an LGA. The accuracy is validated in comparison with the traditional MOM method.

Index Terms — LGA, MM-PO hybrid method, target/rough surface scattering, UV.

I. INTRODUCTION

Electromagnetic scattering from the composite model of a ship on a rough surface is of practical importance to long-range radar surveillance, oceanic remote sensing, and target tracking [1-4]. The low grazing angle (LGA) scattering from the rough surface without a target has been widely studied [5], but the study of target/rough surface scattering under an LGA is much more difficult, because the analysis of these problems is complicated by the many possible interactions between the target and the surface, especially when the target is of arbitrary shape and large electrical size. Some numerical methods based on method of moments have been developed for target/rough surface scattering, e.g., the forward backward method (FBM) [3] and finite element method (FEM) [6]. But the application of the traditional MOM method is restricted when the target and the sea surface are both of large electric scale and is further limited for the LGA incidence. Monte Carlo simulation for scattering from an electrically large ship (ELS) on a rough sea surface under a LGA incidence becomes

impractical because of an extremely large memory large-scale target/ rough surface problems, an efficient method is needed. In our previous studies, a hybrid method MM-PO-UV was introduced to compute the scattering from a target above a sea surface [7].

For ELS on the surface under an LGA, two improvements have been made to this MM-PO-UV hybrid method in this paper. Firstly, the subdivision of the MM and PO region is performed flexibly according to the physical considerations. The MM region contains the ship and a small portion of the neighboring sea surface on the illuminated side where the surface currents need to be modeled accurately in the simulation. Secondly, an iterative solution is applied to solve the large matrix equation caused by the ELS, which is difficult to be solved by direct inversion. To further improve the efficiency, a UV fast algorithm is applied to accelerate the computation during per iterative step. With the two improvements, the method proposed is ideally suited for application to LGA scattering from an arbitrarily shaped target of large electric size on the sea surface.

The remainder of the paper is organized as follows. In section 2, the solution of the improved method is proposed. Then Monte Carlo simulations for bistatic scattering from the composite model of an ELS on a Pierson-Morkowitz rough sea surface at an LGA incidence are demonstrated and discussed in section 3. The results are validated in comparison with the traditional MOM method. Finally, the conclusion is given in section 4.

II. SOLUTION OF THE IMPROVED METHOD

As shown in Fig. 1, a ship is located on the sea surface of length L. Some geometrical parameters will be given later in the computation. For simplicity in explaining the algorithm, the ship and the sea surfaces are assumed to be perfectly conducting and they are illuminated from the left by a TE polarized (with electric field $\hat{y}$ indirection) tapered wave $\vec{E}_i(\vec{r})$ with a tapering parameter g incident along the direction $\vec{k} = k(\hat{x}\sin\theta_i - \hat{z}\cos\theta_i)$, where θ_i is the LGA.

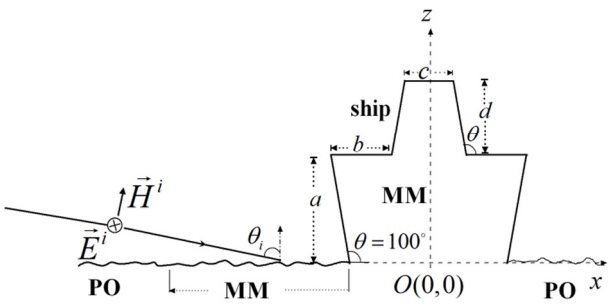

Fig. 1. The model of a ship on rough sea surface.

Within the traditional MM-PO framework, the surface of the scattering model is split into a MM region and a PO region. In our previous research, only the target above the surface is treated as the MM region. For a ship on the rough sea surface, the first improvement made to the hybrid method is to assign the two regions flexibly according to the physical considerations. In this model, the ship target has remarkable induction interaction with the neighboring sea surface on the illuminated side. So the MM region contains not only the ship but also a small portion of the neighboring sea surface where the currents need to be modeled accurately in the simulation. The length of the sea surface in the MM region is an adjustable parameter and set comparable to the height of the ship. This length chosen takes into account all the induction interaction and it won't bring too much computation. The remaining sea surface is considered as the PO region because the re-radiation interaction with the ship is significant in this region, whereas the induction is obvious in the neighboring sea surface. Since a very large sea surface must be included to allow an LGA incidence, the number of current unknowns in the MM region is typically far smaller than the total number of surface current unknowns.

After the subdivision of the MM and PO region is performed, it is possible to follow the similar process in our previous research [7]. Thus, the final matrix equation obtained by constraining the boundary condition in the MM region can be written as:

$$(\overline{\overline{Z}}_{MM,MM} + \overline{\overline{Z}}_{MM,PO} \cdot \overline{\overline{M}}_{PO,MM}) \cdot \bar{I}_{MM} = \bar{V}_{MM}, \quad (1)$$

where $\overline{\overline{Z}}_{MM,MM}$ is the self-impedance matrix of the MM region. $\overline{\overline{Z}}_{MM,PO}$ is the mutual impedance matrix between the currents in the MM region and the PO region. $\overline{\overline{M}}_{PO,MM}$ is called the magnetic-reaction matrix [8] indicating the excitation from the currents in the MM region to the PO region. The dimension of matrices $\overline{\overline{Z}}_{MM,MM}$, $\overline{\overline{Z}}_{MM,PO}$ and $\overline{\overline{M}}_{PO,MM}$ are, $N_{MM} \times N_{MM}$, $N_{MM} \times N_{PO}$, and $N_{PO} \times N_{MM}$, respectively.

For an ELS, N_{MM} becomes large while N_{PO} is much larger than N_{MM} under an LGA incidence. In our former studies [7], the MM-PO-UV method was demonstrated only for an object of moderate size above a rough surface, so the final matrix equation could be solved directly and the UV matrix decomposition technique is mainly combined for the fast filling-in of the matrix elements. When an ELS is presented in this paper, the MM region results in a final matrix equation of large size, which is difficult to be solved by the direct solution. The second improvement in our study is to apply a proper iterative solution to solve the large matrix equation. The well-known BiCGSTAB (ell) [9] is chosen as the iterative solver. Thus, the bottleneck is the calculation of the product of the matrix and a column vector. Then, the UV matrix decomposition techniques could be further combined in the iterative steps.

During per iterative step of the solution, two matrix-vector multiplications $\overline{\overline{Z}}_{MM,MM} \cdot \bar{I}_{MM}$ and $\overline{\overline{Z}}_{MM,PO} \cdot \overline{\overline{M}}_{PO,MM} \cdot \bar{I}_{MM}$ should be calculated. To accelerate the computation of the matrix-vector products, the matrices $\overline{\overline{Z}}_{MM,MM}$, $\overline{\overline{Z}}_{MM,PO}$, and $\overline{\overline{M}}_{PO,MM}$ are considered and replaced by a set of self, near and far interaction sub-matrices in a multilevel way. The multilevel scheme is exactly similar to that proposed for the three-dimensional (3-D) problems in [10]. Each considered matrix is divided into a series of sub-matrix blocks according to the interaction distances. Generally, the rank of the sub-matrix is dependent on the distance between two interaction regions. Therefore, those far interaction sub-matrices with a low rank could be compressed by the UV matrix decomposition technique [11] based on low-rank criterion and interpolation technology.

According to the UV matrix decomposition algorithm, the given far interaction sub-matrix with low rank r could be approximated by the product of a U and V matrix,

$$\overline{\overline{z}}_{m \times n} = \overline{\overline{U}}_{m \times r} \overline{\overline{V}}_{r \times n},$$

where $r << \min(m,n)$. The matrix decomposition is achieved by sampling a small number of rows and columns within the original sub matrix. Therefore, the computational complexity drops from $o(m \times n)$ to $o(r \times (m+n))$ for both the memory requirements and the CPU time consumed in matrix vector multiplication.

The detailed multilevel UV method for the 1-D rough surface scattering had been discussed in [11]. The detailed multilevel UV method for the 3-D problems had been discussed in [10]. In this paper, the multilevel UV method is transformed and applied for 2-D problems. According to the multilevel scheme, the interaction of the matrices $\overline{\overline{Z}}_{MM,PO}$ and $\overline{\overline{M}}_{PO,MM}$ is distinguished as either near interaction or far interaction. Because a large portion of the sea surface is far away from the MM region, most blocks represent the far interaction between the two regions. Only a small portion of the sea surface in the PO region is near the MM region, so the two interaction matrices have a very high compressing ratio by using the multi-level UV method.

III. RESULTS AND DISCUSSIONS

Numerical results are presented and discussed in this section to demonstrate the accuracy and efficiency of this improved method. The validity of the improved method is proved firstly. Then, the method is applied to obtain the LGA scattering from ELS on the sea surface. The results of the large ship case are compared with a smaller one. For all the results, the Pierson-Morkowitz rough sea surface is driven by the wind with a given speed $U = 5 m/s$.

To validate the improved MM-PO-UV hybrid method, simulation results for the composite model under an LGA $\theta_i = 80^o$ are illustrated and compared with the traditional MOM method. In

this validation, the geometrical size of the model is chosen exactly the same as presented in [6]. The surface length is $L = 409.6\lambda$ (λ is the wavelength, $\lambda = 1\,m$) and the tapered wave takes $g = L/6 = 68.2\lambda$. As described in Fig. 1, the electrical size of the ship has $a = 9\lambda$, $b = 5\lambda$, $c = 4\lambda$, $d = 6\lambda$, and $\theta = 100^{\circ}$. The ship geometry is about 15λ high and the deck is 16.1λ wide. The contour of the ship above the sea water has a length of 44.95λ . Considering the height of the ship, a length of 15λ of the sea surface to the left of the ship is considered as the MM region in the improved method.

Figure 2 gives the magnitude of the currents as a function of the length along the contour of the ship from the illuminated side (left side) to the dark side (right side). It is observed that the results of the improved MM-PO-UV hybrid method (the dotted line) and the MOM method (the solid line) are in excellent agreement with each other.

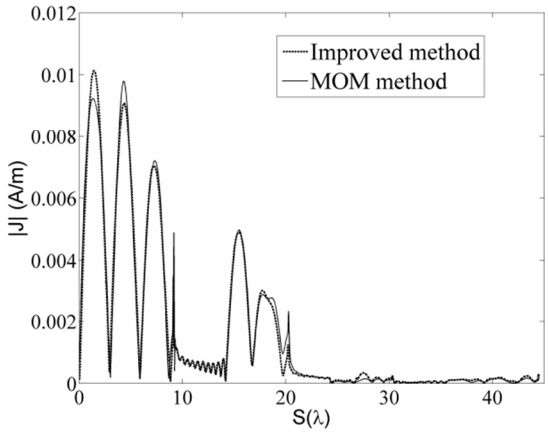

Fig. 2. Comparison of currents on the ship between the improved method and the MOM method .

Figure 3 shows the bistatic scattering results over 50 Monte Carlo realizations of the three methods: MM-PO-UV hybrid method (the dashed line), the improved method (the dotted line), and the MOM method (the solid line). It can be seen that the results of the improved method agree with the MOM method better than the hybrid method without improvements.

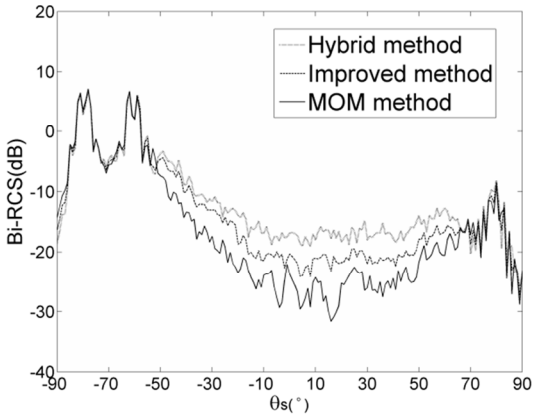

Fig. 3. Comparison of bistatic scattering for three methods.

For comparison, the main memory requirements and the computational time of the three methods in Fig. 3 are given in Table 1. It could be concluded that the improved method has better accuracy when its requirements for the computational resources remain almost the same as the hybrid method.

Table 1: Memory requirements and relative computational time

Method	**Unknowns**	**Memory(MB)**	**Time(s)**
MOM	3804	197	690
Improved	745	44	42
Hybrid	620	42	29

The composite model scattering feature has positive correlation with the shape characteristic of the ship and the distribution of the sea surface. As shown in Fig. 1, the ship's hull forms a large 80^{o} corner reflector with respect to the flat sea surface. The deck house on top of the ship makes a 100^{o} corner reflector with the sea surface. Considering the incident angle from the left, strong interactions exist between the near-specular directions of the corner reflectors. It is of interest to see how the coupling interactions contribute to the scattering.

The specular reflection of the corner reflectors formed by the ship and the sea is illustrated in Fig. 4. Figure 4(a) indicates the backscattering path, which involves two reflections from the sea surface and one bounce from the ship's hull. Figure 4 (b) shows the backward scattering in the

direction $\theta_s = -60^o$ contributed by two different paths. Both the two paths involve a reflection from the sea surface and a bounce from the ship.

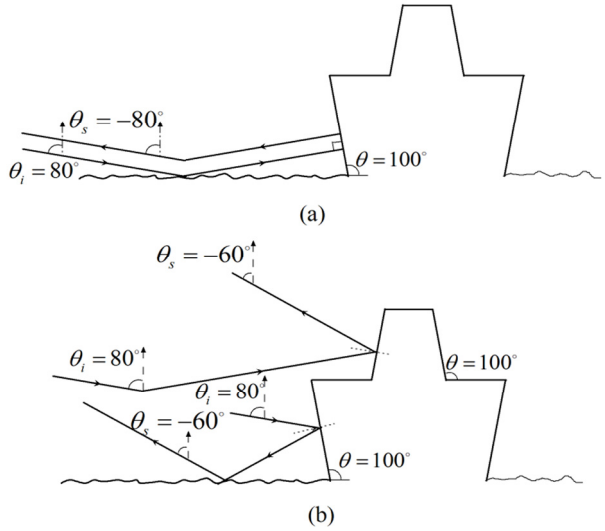

Fig. 4. Specular reflection of the corner reflectors between the ship and the sea surface.

Compared with the corner reflectors formed by the sea surface, the deckhouse also forms a 100^o corner reflector with the deck itself, which is much smaller. The physics of scattering waves interpreted in Fig. 5 (a) indicates that the return wave contributes to the direction $\theta_s = -60^o$. In Fig. 5 (b), the incidence is reflected by the deckhouse directly because its direction is normal to the left of the deckhouse on the top.

Due to the specular and diffuse reflection, it is expected that the corner reflectors will give rise to a very high RCS in the near-specular directions over a wide degrees range. As expected, the RCS in Fig. 3 is greatly enhanced over a broad range of scattering degrees $\Delta\Phi$ ($\Delta\Phi = [-85^\circ, -55^\circ]$) due to the strong interactions between the ship and the sea. The forward near-specular scattering is also strong over the degree range $\Delta\Psi$ ($\Delta\Psi = [75^\circ, 85^\circ]$). The improved hybrid method matches well with the traditional MOM method over the range $\Delta\Phi$ and $\Delta\Psi$, which is of great interest in the practical engineering problems. The peak at forward direction and the backward peaks match exactly well with the traditional MOM method because the PO approximation shows more accuracy in this near-specular directions.

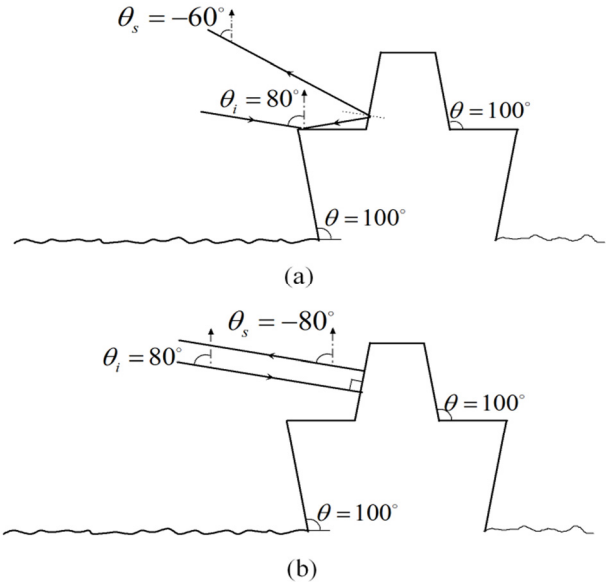

Fig. 5. Specular reflection by the ship itself.

Under the LGA incidence, selection of g and L should be large enough to ensure the convergence. However, a much longer surface results in a huge number of current unknowns, which makes the computation impractical. Previously, no numerical results have been reported involving a rough sea surface much larger than $L = 409.6\lambda$ applied in this composite model. In this paper, a much larger g and L is selected to make sure the ratio of the illuminated intensity on the target to the tapered wave peak can reach to 0.94 [13]. The tapered wave control parameter is chosen as follows:

$$g = 4(r/\cos\theta_i + h\tan\theta_i). \qquad (2)$$

For the composite model in our study, r is the maximum radius of the ship circled by the dotted line in Fig. 6 , h corresponds to the height of the circle center. θ_i is the incidence angle. We have $r = 11\lambda$, $h = 7.5\lambda$ computed in this case, and a $g = 423.7\lambda$ is calculated according to Eq. (2) .

Figure 7 compares the scattering from the composite model with different g and L but with the same other parameters given in the validation.

(1) $g = 68.2\lambda$; $L = 409.6\lambda$;

(2) $g = 423.7\lambda$; $L = 4g = 1694\lambda$;

(3) $g = 423.7\lambda$; $L = 6g = 2542\lambda$.

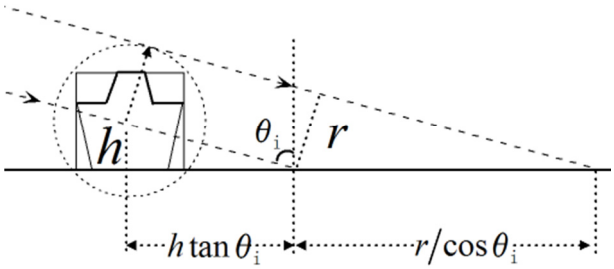

Fig. 6. Sufficient illumination by the tapered wave under an LGA.

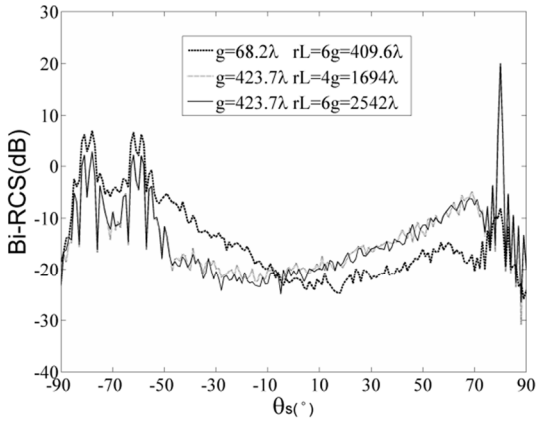

Fig. 7. Bistatic scattering of the same ship with different g and L .

It can be seen that the scattering results for the small $g = 68.2\lambda$, $L = 409.6\lambda$ is not convergent in Fig. 7. That's because when under an LGA incidence, not only the sea region interacting with the ship is greatly enlarged, but also the primary scattering of the ship in the forward direction reaches a much farther area of the sea surface. Obviously, the composite model is not fully illuminated by the incident tapered wave with $g = 68.2\lambda$. But it is observed that when g is chosen large enough to ensure the illumination, then a surface length of $L = 4g$ is sufficient for the simulation.

In the following, this proposed method in our study is applied to a large ship case calculating the LGA scattering from ELS on a sea. The numerical results are compared with a smaller ship case. The smaller ship case has parameters:

$a = 9\lambda, b = 5\lambda, c = 4\lambda, d = 6\lambda$; $g = 423.7\lambda$, $L = 4g = 1694\lambda$.

The large ship case has parameters:

$a = 36\lambda$, $b = 20\lambda$, $c = 16\lambda$, $d = 24\lambda$; $g = 1694\lambda$, $L = 4g = 6779\lambda$.

The large ship is about 60λ high and the deck is 64.4λ wide. The contour of the ship above the sea water has a length of 179.8λ . The MOM region contains the ship and a small portion of the nearby sea surface with a length of 60λ . A sampling of 10 points per wavelength will result in 1798 ship surface current unknowns and a total of 67790 rough surface current unknowns. The large number of unknowns would be prohibitive for standard approaches to the MOM, especially if a three-dimensional problem must be considered. Applying the improved MM-PO-UV hybrid method, the final matrix equation is of size 2398, which is far smaller than the unknowns used in the MOM method but still difficult to be solved directly. This proposed method makes it possible for the simulation of scattering from an electrically large ship on an extremely large-scale sea surface.

Comparison is made between the smaller ship case and the large ship case in Fig. 8. It is shown that the RCS is strong over a range of near-specular degrees $\Delta\Phi$ ($\Delta\Phi = [-85^\circ, -55^\circ]$) for both cases. But the strong RCS results split for the smaller ship case in the scattering angles $\theta_s = -80^\circ$ and $\theta_s = -60^\circ$ where the RCS reach sharp peaks for the large ship case. To explain this phenomenon, the total scattering from the composite model can be decomposed into two scattering terms: 1) the ship term refers to the scattering contributed by the radiation of currents on the ship; 2) the sea term means the scattering contributed by the radiation of currents on the sea surface.

Figure 9 compares the two decomposed scattering terms of the smaller ship case. It is noticed obviously that the sea term is stronger than the ship term over $\Delta\Phi$ ($\Delta\Phi = [-85^\circ, -55^\circ]$), which is the near-specular directions. The backward scattering over $\Delta\Phi$ is dominated by the sea term due to the re-radiation interaction from the ship.

Compared with the smaller ship case in Fig. 9, each scattering term in Fig. 10 for the large ship case is greatly enhanced over the range $\Delta\Phi$. That's because as the electrical size of the ship is increased, the sea regions interacting with the ship become larger. Thus, the coupling interaction between the large ship and a wider area of the sea surface is apparently stronger than the smaller ship case, which gives rise to higher RCS in the near-specular directions. As a result of the large size, the ship term is greatly intensified and it has a very close value to the sea term in the backscattering.

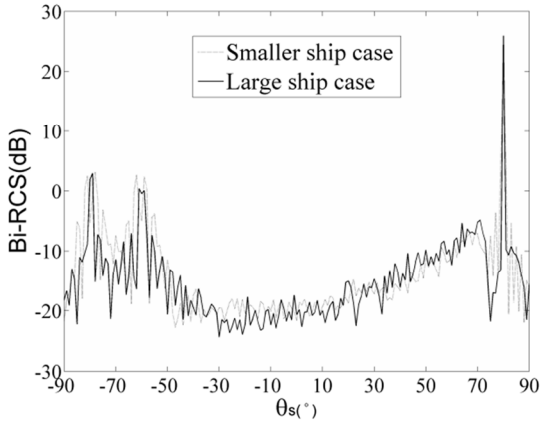

Fig. 8. Comparison of bistatic scattering between a large ship case and a smaller ship case.

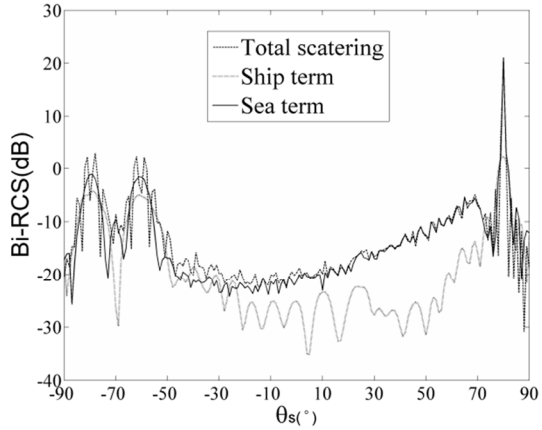

Fig. 9. Scattering terms of the smaller ship case.

To explain the two backward splits of the small ship case, the phase of the scattered field contributed by each scattering term is extracted, respectively. Taking the split in $\theta_s = -80^\circ$ as an example, the phase of the ship term is -60° and the sea term is 90.1°. There's a phase difference of about $\Delta\varphi = 150.1^\circ$ between the two scattering terms. Although each scattering term reaches a high value in the backscattering angle $\theta_s = -80^\circ$ respectively, the total scattering is reduced due to the nearly opposite phase of the two scattering terms. The phase difference could reduce the scattering but it will also enhance the total scattering results. Different to the smaller ship case, the RCS of the large ship case in the backscattering is greatly strengthened, because of the nearly same phase.

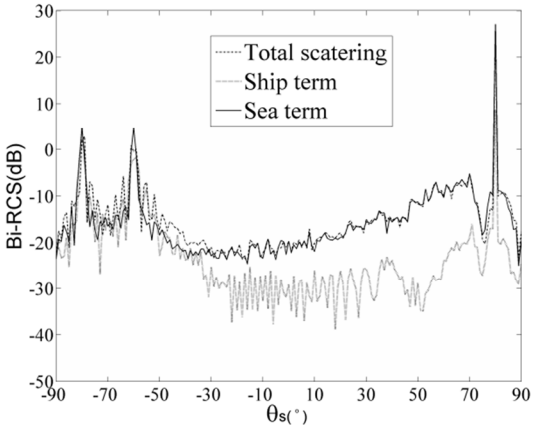

Fig. 10. Scattering terms of the large ship case.

Furthermore, energy conservation by integrating bistatic scattering over the upper half space is given in [11]:

$$P = \int_{-\frac{\pi}{2}}^{\frac{\pi}{2}} d\theta_s \sigma(\theta_s). \tag{3}$$

In our simulations, the value calculated is close to the unity. The accuracy of the algorithm for the energy conservation is validated.

IV. CONCLUSION

With the improvements made to the hybrid method, its scope of application is enhanced for complex large-scale problems such as an arbitrarily shaped ship target of large electrical scale on the surface under an LGA. In this study, the subdivision of the MM and PO region is performed flexibly according to the physical considerations. An iterative solution combining the UV decomposition method is applied to solve the large matrix equation. The accuracy of the

proposed method was validated by the comparison made with the MOM method. As the large number of unknowns would be prohibitive for standard approaches to the MOM, the efficient hybrid method makes it possible for large-scale complex problems, and the large number of simulations can be handled in a reasonable amount of time.

ACKNOWLEDGMENT

This work is supported by the National Natural Science Foundation of China under Grant No. 61001059, by the China Postdoctoral Science Foundation, and by the Fundamental Research Funds for the Central Universities.

REFERENCES

[1] E. A. Shtager, "An Estimation of Sea Surface Influence on Radar Reflectivity of Ships," *IEEE Transactions on Antennas and Propagation*, vol. 47, no. 10, pp. 1623-1627, Oct. 1999.

[2] R. J. Burkholder, M. R. Pino, and F. Obelleiro, "A Monte Carlo Study of the Rough Sea Surface Influence on the Radar Scattering from 2-D Ships," *IEEE Transactions on Antennas and Propag. Mag.*, vol. 43, no. 2, 25-33, Apr. 2001.

[3] M. R. Pino, R. J. Burkholder, and F. Obelleiro, "Spectral Acceleration of the Generalized Forward-Backward Method," *IEEE Trans. Antennas Propag.*, vol. 50, no. 6, pp. 785-797, Jun. 2002.

[4] K. Jamil and R. J. Burkholder, "Radar Scattering from a Rolling Target Floating on a Time-Evolving Rough Sea Surface," *IEEE Trans. Geosci. Remote Sens.*, vol. 44, no. 11, pp. 3330-3337, 2006.

[5] C. H. Chan, L. Tsang, and Q. Li, "Monte Carlo Simulations of Large-Scale One Dimensional Random Rough-Surface Scattering at Near Grazing Incidence: Penetrable Case," *IEEE Trans. Antennas Propag.*, vol. 46, no. 1, pp. 142–149, Jan. 1998.

[6] P. Liu and Y. Q. Jin, "Numerical Simulation of Bistatic Scattering from a Target at Low Altitude above Rough Sea Surface under an EM-Wave Incidence at Low Grazing Angle by using the Finite Element Method," *IEEE Trans. Antennas Propag.*, vol. 52, no. 5, pp. 1205-1210, May 2004.

[7] S. Y. He and G. Q. Zhu, "A Hybrid MM-PO Method Combining UV Technique for Scattering from Two-Dimensional Target above a Rough Surface," *Microwave Opt. Technol. Lett.*, vol. 49, no. 12, pp. 2957-2960, Dec. 2007.

[8] H. T. Chen, J. X. Luo, and G. Q. Zhu, "Using UV Technique to Accelerate the MM-PO Method for Three-Dimensional Radiation and Scattering Problem," *Microwave Opt. Technol. Lett.*, vol. 48, no. 8, pp. 1615 -1618, 2006.

[9] E. Topsakal, R. Kindt, K. Sertel, and J. Volakis, "Evaluation of the BiCGSTAB(l) Algorithm for Finite-Element/Boundary-Integral Method," *IEEE Trans. Antennas Propagation Magazine*, vol. 43, no. 6, pp. 124-131, Dec. 2001.

[10] F. S. Deng, S. Y. He, H. T. Chen, W. D. Hu, W. X. Yu, and G. Q. Zhu, "Numerical Simulation of Vector Wave Scattering from the Target and Rough Surface Composite Model with 3-D Multilevel UV Method," *IEEE Trans. Antennas Propagat*., vol. 58, no. 5, pp. 1625-1634, May 2010.

[11] L. Tsang, D. Chen, P. Xu, Q. Li, and V. Jandhyala, "Wave Scattering with the UV Multilevel Partitioning Method: 1. Two-Dimensional Problem of Perfect Electric Conductor Surface Scattering," *Radio Science*, vol. 39, RS5010, Oct. 2004.

[12] L. Tsang, J. A. Kong, K. H. Ding, and C. O. Ao, *Scattering of Electromagnetic Waves, Numerical Simulations*, Wiley-Interscience, Hoboken, N. J., 2001.

[13] H. X. Ye and Y. Q. Jin, "Fast Iterative Approach to Difference Scattering from the Object above a Rough Surface," *IEEE Trans. Geosci. Remote Sens*., vol. 44, no. 1, pp. 108-115, Jan. 2006.

S. Y. He was born in 1982. She received the telecommunication engineering degree and the Ph.D. degree in Radio Physics from Wuhan University, Wuhan, China, in 2003 and 2009, respectively. She is currently a post doctoral researcher at Wuhan University. From 2005 to 2006, she was a Research Assistant in Wireless Communications Research Centre,

City University of Hong Kong. Her research interests include EM theory and its application, computational electromagnetic, and radar imaging.

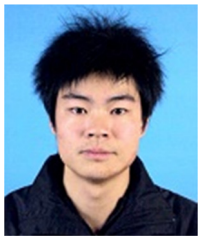

C. Li was born in 1986. He received the B.S. degree in Information Countermeasure Technology from North University of China, China, in 2008. He is currently working towards the Ph.D. degree in Radio Physics at Wuhan University, Wuhan, China. His current research interests are in numerical methods in electromagnetism, inverse scattering, electromagnetic scattering, and radiation.

F. Zhang was born in 1986. She received the telecommunication engineering degree from Wuhan University, Wuhan, China, in 2009. She is currently working towards the Ph.D. degree in Radio Physics at Wuhan University, Wuhan, China. Her current research interests include electromagnetic scattering and complex objects characterizing.